Differential Movement across Byrd Glacier, Antarctica, as indicated by Apatite (U–Th)/He thermochronology and geomorphological analysis

Article · January 2016

DOI: 10.6084/M9.FIGSHARE.3453494

5 authors, including:

Daniel J. Foley
United States Geological Survey
11 PUBLICATIONS **18** CITATIONS
SEE PROFILE

Edmund Stump
Arizona State University
54 PUBLICATIONS **1,941** CITATIONS
SEE PROFILE

Matthijs van Soest
Arizona State University
148 PUBLICATIONS **1,884** CITATIONS
SEE PROFILE

Kip Hodges
Arizona State University
436 PUBLICATIONS **18,082** CITATIONS
SEE PROFILE

Differential Movement across Byrd Glacier, Antarctica, as indicated by Apatite (U–Th)/He thermochronology and geomorphological analysis

D. J. FOLEY, E. STUMP*, M. VAN SOEST, K. X. WHIPPLE & K. V. HODGES

School of Earth and Space Exploration, Arizona State University, Tempe, AZ 85287, USA

**Corresponding author (e-mail: ed.stump@asu.edu)*

Abstract: The objectives of this study were to assess possible differential movement across an inferred fault beneath Byrd Glacier, and to measure the timing of unroofing in this portion of the Transantarctic Mountains. Apatites separated from rock samples collected from known elevations at various locations north and south of Byrd Glacier were dated using single crystal (U–Th)/He analysis. Results indicate a denudation rate of *c.* 0.04 mm a^{-1} in the time range *c.* 140–40 Ma. Distinct age v. elevation plots from north and south of Byrd Glacier indicate an offset of *c.* 1 km across the glacier with south side up. A Landsat image of the Byrd Glacier area was overlain on an Aster Global Digital Elevation Model and spot elevations of the Kukri erosion surface to the north and south of Byrd Glacier were mapped. The difference in elevation of the erosion surface across Byrd Glacier also shows an offset of *c.* 1 km with south side up. Results support a model of relatively uniform cooling and unroofing of the region with later, post-40 Ma fault displacement that uplifted the south side of Byrd Glacier relative to the north.

Supplementary material: Sample and apatite (U–Th)/He data are listed at http://www.geolsoc.org.uk/SUP18671

Byrd Glacier, one of the major outlet glaciers crossing the Transantarctic Mountains (Fig. 1), marks a major discontinuity in the Neoproterozoic–early Palaeozoic Ross orogen, with plutonics and upper amphibolite-grade metamorphics to the north and lower greenschist-grade metamorphics and limestones to the south, indicating considerable differential unroofing of the orogen prior to deposition of the Beacon Supergroup on the Kukri erosion surface (Stump *et al.* 2005). Grindley & Laird (1969) mapped post-Beacon faults beneath Byrd Glacier and other outlet glaciers in the region, but cited no evidence other than the presence of the glaciers themselves.

This study asked the question, whether there are indications of displacement across the inferred Byrd fault, and if yes, what the amount of throw was. To assess possible differential movement across Byrd Glacier, we have used a two-pronged approach combining thermochronology, (U–Th)/He analysis of apatite and geomorphology, comparing elevations of the Kukri erosion surface on the north and south sides of Byrd Glacier.

Background

Our understanding of the history of uplift and denudation of the Transantarctic Mountains is based primarily on low-temperature thermochronological studies using apatite fission track analysis of samples collected from 'vertical profiles' (Gleadow & Fitzgerald 1987; Fitzgerald & Gleadow 1988; Fitzgerald 1992; Fitzgerald & Stump 1997; Lisker 2002). The Transantarctic Mountains are ideally suited for such studies because magmatism throughout the entirety of the range occurred in a brief period during the Jurassic (Fleming *et al.* 1997), totally annealing older fission tracks, except at two known localities where Palaeozoic apatite fission track ages survive (the western, inland margin of northern Victoria Land (Fitzgerald & Gleadow 1988) and the Miller Range at the inland margin of the central Transantarctic Mountains (Fitzgerald 1994)). When data are plotted on age v. elevation diagrams, they indicate that exhumation of the entire Transantarctic Mountains began in the Early Cenozoic, ranging between 45 and 55 Ma depending on the region. The central Transantarctic Mountains and the Scott Glacier area also have indications of pulses of exhumation in the Cretaceous (Stump & Fitzgerald 1992; Fitzgerald 1994).

One study utilizing (U–Th)/He analysis was conducted in the Ferrar Glacier area of southern Victoria Land where vertical profiles have been analysed on opposite sides of the glacier (Fitzgerald *et al.* 2006). Although the data are very scattered, probably because of a variety of complications

From: HAMBREY, M. J., BARKER, P. F., BARRETT, P. J., BOWMAN, V., DAVIES, B., SMELLIE, J. L. & TRANTER, M. (eds) 2013. *Antarctic Palaeoenvironments and Earth-Surface Processes*. Geological Society, London, Special Publications, **381**, 37–43. First published online August 6, 2013, http://dx.doi.org/10.1144/SP381.25

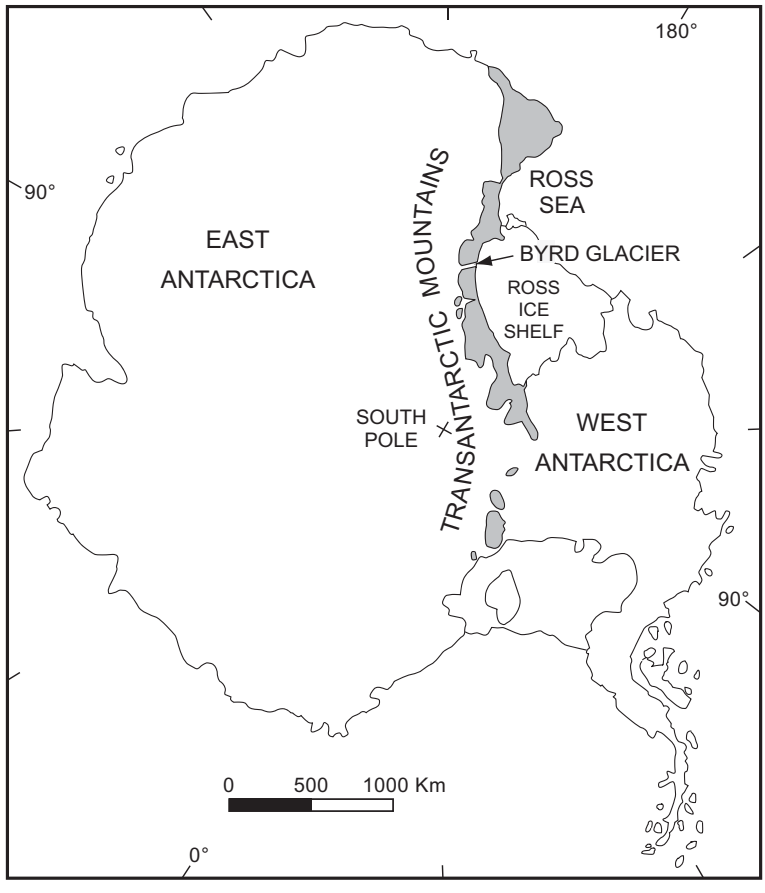

Fig. 1. Location map, Byrd Glacier.

associated with the technique, in general they indicate slow cooling in the Late Cretaceous and an increased cooling rate in the early Cenozoic.

(U–Th)/He thermochronology

Analytical procedures

The (U–Th)/He dating method is based on the production of ^{4}He nuclei (α particles) by uranium and thorium series as well as ^{147}Sm decay (Zeitler *et al.* 1987; Farley 2002). The helium closure temperature for apatite is *c.* 70 °C, making this method well suited for quantifying the cooling history of rocks as they pass through the upper 1–3 km of the crust (Reiners & Farley 2001; Ehlers & Farley 2003).

We chose eight samples of igneous and metamorphic rocks with known elevations from north and south of Byrd Glacier (Table 1, Fig. 2). The elevation of rock samples ESPR and JIF are estimated to be accurate within 10 m based on helicopter altimeter readings at the collecting sites. Elevations of the other rocks are based on mapping localities on the base map with a 200 m contour interval and are estimated to be accurate within 50 m.

In order to extract apatites for analysis, standard crushing, magnetic and heavy liquid separation

Table 1. *Sample and apatite (U/Th)/He data*

Rock	Side	Elevation (m)	Elevation error (m)	Apatite mean age (Ma)
ESPR	North	3450	10	142.9 ± 17.5
JIF	North	1800	10	102.1 ± 9.3
JIP	North	800	50	52.8 ± 18.0
JID	North	600	50	69.2 ± 18.2
JMG	North	200	50	50.5 ± 6.8
JHG	South	1750	50	54.2 ± 16.6
JHI	South	1700	50	53.9 ± 19.2
JMZ	South	1150	50	39.3 ± 14.5

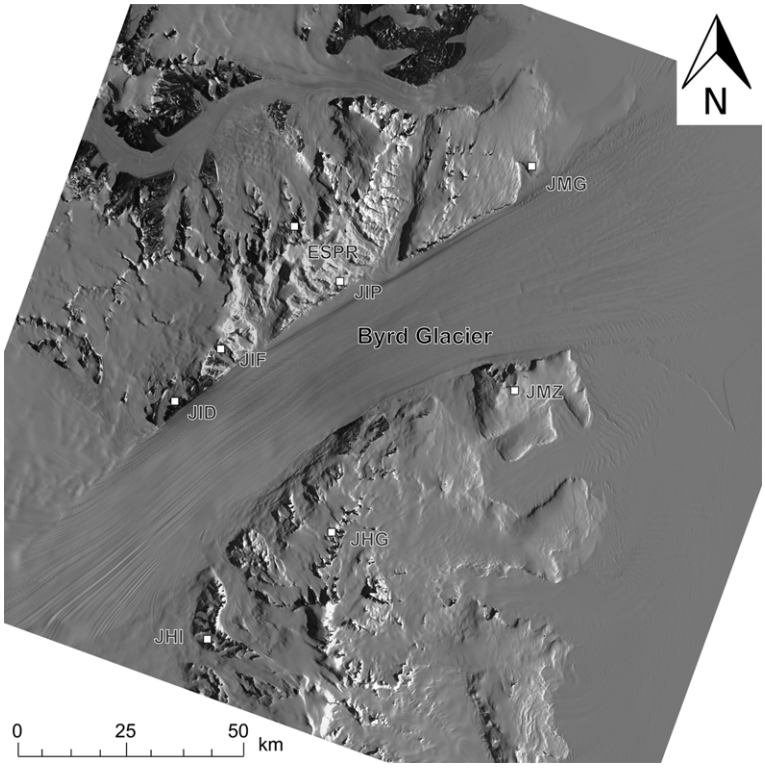

Fig. 2. Sample locations, Byrd Glacier area.

procedures were conducted on the samples. Separated grains were then hand-picked under a binocular microscope on the basis of morphology, size, clarity, euhedral crystal shape and lack of optically detectable inclusions. At least five apatite crystals from each sample were dated following procedures described in Schildgen *et al.* (2009) and updated in van Soest *et al.* (2011). These involved releasing helium by laser heating of apatite grains in an ASI Alphachron and spiking the gas with ^{3}He for ^{4}He/^{3}He analysis in the Noble Gas Geochemistry and Geochronology Laboratory at Arizona State University. Next, apatites were dissolved and solutions were analysed for uranium and thorium with an Thermo X series quadrupole inductively coupled plasma mass spectrometer in the W. M. Keck Foundation Laboratory for Environmental Geochemistry at Arizona State University. Ages were then calculated with an iterative process using blank corrected helium, thorium and uranium values.

Results

Mean (U–Th)/He ages are given in Table 1. The mean age for the suite of apatites from each rock sample is listed along with 2σ errors, which range from 39 ± 15 to 143 ± 18 Ma. The complete apatite (U–Th)/He dataset is available as Supplementary Material. To assess cooling histories and derive exhumation rates, all data were plotted in an age v. elevation diagram (Fig. 3) and a least squares regression through the data was computed in Matlab utilizing the equations of York (1969). The age variable was regressed using 2σ error uncertainties for each data point and a mean squared weighted deviation (MSWD) value was derived. From the slope of the derived regression equation for all apatite data, the exhumation rate between *c.* 140 and 40 Ma is 0.04 ± 0.01 (2σ) mm a^{-1} with a mean squared weighted deviation of 8.39.

To further assess cooling histories and possible differential movement north and south of Byrd Glacier, the apatite age v. elevation data from north and south of Byrd Glacier were regressed separately. The least squares regression of the data from north of Byrd Glacier indicates an exhumation rate of 0.035 ± 0.006 mm a^{-1} between *c.* 140 and 50 Ma with a mean squared weighted deviation of 0.93 (Fig. 4). Least squares regression of the data from south of Byrd Glacier indicates an

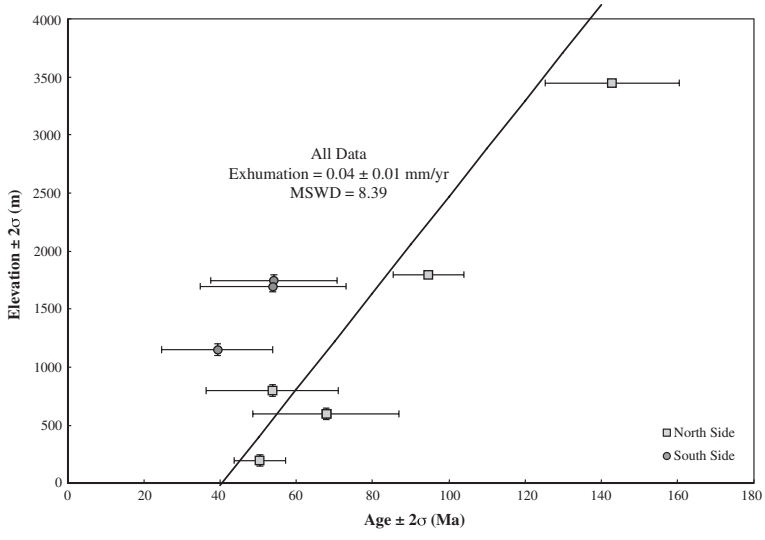

Fig. 3. Total apatite age v. elevation plot. Error bars are 2σ.

exhumation rate of 0.04 ± 0.05 mm a^{-1} between *c.* 55 and 40 Ma with a mean squared weighted deviation of 0.006 (Fig. 4). Separation of apatite age v. elevation data from north and south of Byrd Glacier produces exhumation rates similar to that derived from the total sample set, but separating the two sets of data leads to improved mean squared weighted deviation values.

When comparing apatite (U–Th)/He data across Byrd Glacier, Figure 4 shows that at similar elevations ages from the south are younger than ages from the north and at similar ages sample elevations from south of the glacier are higher than those from north of the glacier, indicating differential movement across Byrd Glacier. Two models could plausibly explain this inferred differential movement. In the first model, a relatively uniform exhumation across Byrd Glacier is followed by later fault displacement. The second model involves differential exhumation with the

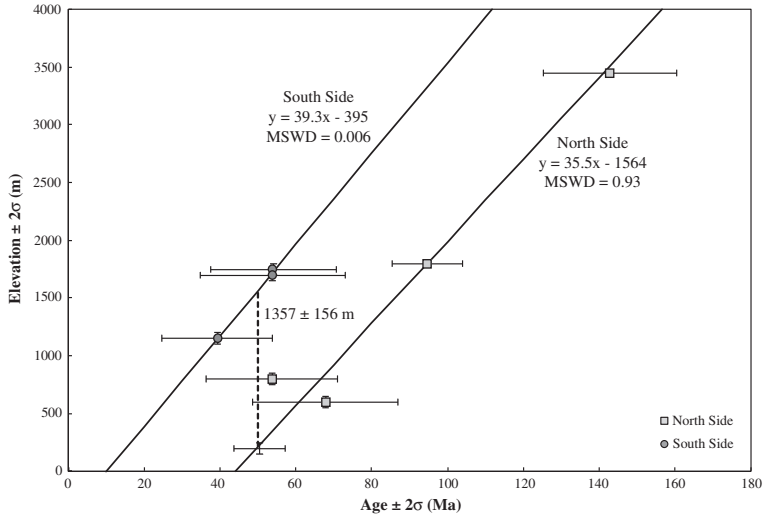

Fig. 4. Apatite age v. elevation plot with data separated between north (squares) and south (circles) samples. Bold lines are least squares regressions. Error bars are 2σ. Offset at the 50 Ma datum is plotted as a dashed line.

south side exhumed at a more rapid rate than the north side. The exhumation rates inferred from apatite data across Byrd Glacier are identical within error, 0.035 ± 0.006 mm a^{-1} to the north and 0.04 ± 0.05 mm a^{-1} to the south, suggesting that the differential movement was more probably attributable to an offset from fault displacement.

In order to quantify offset across Byrd Glacier, regression line equations of apatite age v. elevation data from north and south of Byrd Glacier were compared to calculate the difference in elevation (Fig. 4). The regression line equations of $y = 35.5x - 1564$ and $y = 39.3x - 395$, respectively, north and south of Byrd Glacier were utilized in calculations, with y representing elevation and x representing age. Offset was calculated by inputting an age value x as the predictor variable into each regression equation, resulting in a predicted elevation value for a given age. Then the north side elevation was subtracted from the south to determine the difference in elevation of the inferred rock at the same age across Byrd Glacier. The apatite data across Byrd Glacier is well constrained for comparison in the range of *c.* 40–60 Ma as rocks in this age range are represented in both north and south datasets. Therefore, an age value of 50 Ma was used for x in both north and south regression equations. The resulting elevation difference across Byrd Glacier is 1357 ± 156 (2σ) m.

Geomorphology

Analytical procedures

For assessing possible differential movement in this area from a geomorphological standpoint, the Kukri erosion surface was chosen as a datum, with the assumption that at the time of its formation the erosion surface had a relatively uniform elevation. The objective was to determine the current elevation of the Kukri erosion surface north and south of Byrd Glacier in order to quantify any displacement.

To map the elevation of the Kukri erosion surface across Byrd Glacier, imagery from the 30 m resolution Landsat Image Mosaic of Antarctica was draped over the 30 m resolution Aster Global Digital Elevation Model of the region. These were

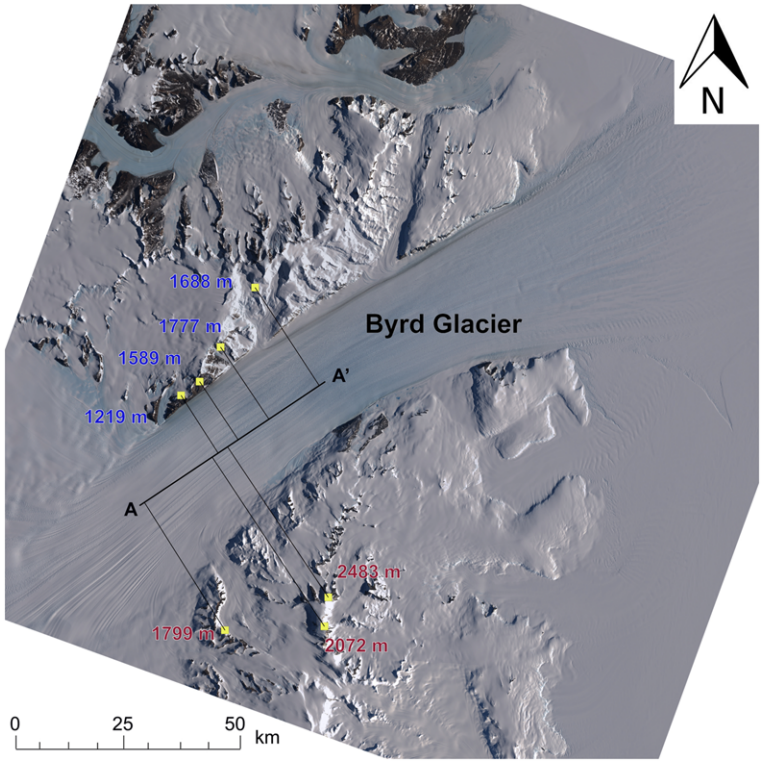

Fig. 5. Locations of Kukri erosion surface with corresponding elevations plotted on Byrd Glacier digital elevation model overlain with Landsat image. Note that distance values in Figure 6 and Table 2 are measured from the A end of the A–A′ transect, where the projection of the 1799 m elevation intersects the transect.

Table 2. *Kukri elevation and distance data*

N distance (m)	Elevation N (m)	S distance (m)	Elevation S (m)
20 677	1219	0	1799
27 404	1589	17 671	2072
33 679	1777	22 767	2483
45 087	1688		

N distance and S distance are measured from the A end of the A–A′ transect, where the projection of the 1799 m elevation intersects the transect.

processed in Arc Geographic Information System programs, Arc Map, Arc Scene and Arc View.

Based on field photographs, the Kukri erosion surface was located at seven points on Landsat imagery of the area, four points on the north side of Byrd Glacier and three points on the south side as shown in Figure 5. From these locations, elevations were extracted from the digital elevation model. Orthogonal projections of these points were then made onto a transect parallel to Byrd Glacier. The distances between points on transect A–A′ are measured from the southwesternmost point of the transect (Fig. 5).

Results

Elevation and distance data is presented in Table 2 and plotted in Figure 6, revealing that the observed points on the Kukri erosion surface are at higher elevations on the south side relative to the north. In addition, both north and south points show elevations higher in the east, indicating a slight dip toward the west. In order to accurately compare the elevation of the projected erosion surface across Byrd Glacier, the dips were calculated with a least-squares regression. The results are west dips of the Kukri erosion surface of 1.79° on the north side and 1.81° on the south side of Byrd Glacier.

As the dips of the erosion surface differ by only 0.02°, where the projections of the erosion surface overlap on the A–A′ transect, the elevation of the erosion surface across Byrd Glacier can be compared. However, this does involve the uncertainties of assuming the erosion surface has consistent strikes across Byrd Glacier and is not significantly deformed. The strikes could not be assessed in this study as locations of the Kukri erosion surface could not be extended farther north and south of the measured points owing to limited visible exposure and no available on-site data.

To measure the offset of the Kukri erosion surface, the elevation difference was calculated across Byrd Glacier by comparing the erosion surface elevations on either side at a point where the traces of the erosion surface overlap (Fig. 6). The erosion surface elevation data across Byrd Glacier overlap along the A–A′ transect between *c.* 20.7 and 22.7 km; therefore, a distance value of 21.7 km was chosen. The derived regression

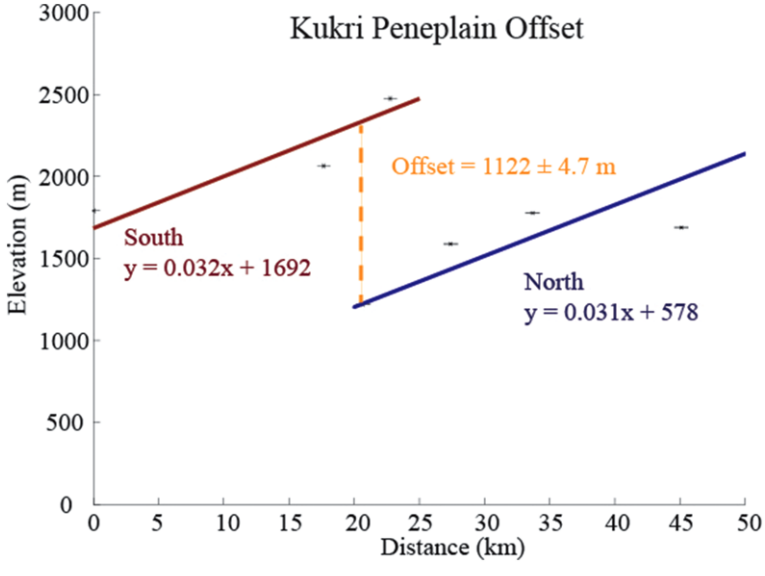

Fig. 6. Plot of projections of elevation data from Kukri erosion surface separated between north (blue) and south (red) points. Bold lines are least squares regressions of the points. Offset at the 21.7 km distance (measured from A on the A–A′ transect) is plotted in yellow.

equations from the Kukri erosion surface were $y = 0.0312x + 578$ (north side) and $y = 0.0316x + 1692$ (south side) with y representing elevation and x representing distance. Elevations were calculated based on an x value of 21.7 km as the predictor. At this location the calculated difference in elevation of the Kukri erosion surface across Byrd Glacier is 1122 ± 4.7 (2σ) m.

Whereas the offset in elevations of the Kukri erosion surface could be interpreted as due to horizontal displacement along a strike-slip fault, the thermochronologic data indicate that the dominant element of movement is vertical uplift.

Conclusions

Both thermochronologic and geomorphologic data indicate that the south side of Byrd Glacier was displaced upward relative to the north side, supporting the original suggestion by Grindley & Laird (1969) that a fault exists beneath Byrd Glacier. A comparison of offset as indicated by apatite (U–Th)/He thermochronologic and geomorphologic data demonstrates a close correspondence in the amount of vertical differential movement, 1357 ± 156 v. 1122 ± 4.7 m. The results suggest a model of relatively uniform exhumation followed by fault displacement. The thermochronological data suggest that the timing of the fault displacement occurred sometime after *c.* 40 Ma.

The authors would like to acknowledge B. Adams for his help with the MATLAB coding. NSF grant OPP 9909463 funded collection of the samples used in this study. F. Lisker and M. Laird are thanked for their helpful reviews.

References

EHLERS, T. A. & FARLEY, K. A. 2003. Apatite (U–Th)/He thermochronometry: methods and applications to problems in tectonic and surface processes. *Earth and Planetary Science Letters*, **206**, 1–14.

FARLEY, K. A. 2002. (U–Th)/He dating: techniques, calibrations, and applications. *Noble Gas Geochemistry, Reviews in Mineralogy and Geochemistry*, **47**, 819–843.

FITZGERALD, P. G. 1992. The Transantarctic Mountains of southern Victoria land: the application of apatite fission track analysis to a rift shoulder uplift. *Tectonics*, **11**, 634–662.

FITZGERALD, P. G. 1994. Thermochronologic constraints on post-Paleozoic tectonic evolution of the central Transantarctic Mountains, Antarctica. *Tectonics*, **13**, 818–836.

FITZGERALD, P. G. & GLEADOW, A. J. W. 1988. Fission-track geochronology, tectonics and structure of the Transantarctic Mountains in Northern Victoria land, Antarctica. *Chemical Geology: Isotope Geoscience*, **73**, 169–198.

FITZGERALD, P. G. & STUMP, E. 1997. Cretaceous and Cenozoic episodic denudation of the Transantarctic Mountains, Antarctica: new constraints from apatite fission track thermochronology in the Scott Glacier region. *Journal of Geophysical Research*, **102**, 7747–7765.

FITZGERALD, P. G., BALDWIN, S. L., WEBB, L. E. & O'SULLIVAN, P. B. 2006. Interpretation of (U–Th)/He single grain ages from slowly cooled crustal terranes: a case study from the Transantarctic Mountains of southern Victoria land. *Chemical Geology*, **225**, 91–120.

FLEMING, T. H., HEIMANN, A., FOLAND, K. A. & ELLIOT, D. H. 1997. $^{40}Ar/^{39}Ar$ geochronology of Ferrar Dolerite sills from the Transantarctic Mountains, Antarctica: implications for the age and origin of the Ferrar magmatic province. *Geological Society of America Bulletin*, **109**, 533–546.

GLEADOW, A. J. W. & FITZGERALD, P. G. 1987. Uplift history and structure of the Transantarctic Mountains: new evidence from fission track dating of basement apatites in the Dry Valleys area, southern Victoria land. *Earth and Planetary Science Letters*, **82**, 1–14.

GRINDLEY, G. W. & LAIRD, M. G. 1969. *Geology of the Shackleton coast*. American Geographical Society, Antarctic Map Folio Series, Folio 12, Sheet XIV.

LISKER, F. 2002. Review of fission studies in northern Victoria Land, Antarctica – passive margin evolution v. uplift of the Transantarctic Mountains. *Tectonophysics*, **349**, 57–73.

REINERS, W. & FARLEY, K. A. 2001. Influence of crystal size on apatite (U–Th)/He thermochronology: an example from the Bighorn Mountains, Wyoming. *Earth and Planetary Science Letters*, **188**, 413–420.

SCHILDGEN, T. F., EHLERS, T. A., WHIPP, D. M. JR, VAN SOEST, M. C., WHIPPLE, K. X. & HODGES, K. V. 2009. Quantifying canyon incision and Andean Plateau surface uplift, southwest Peru: a thermochronometer and numerical modeling approach. *Journal of Geophysical Research, Earth Surface*, **114**, F04014, doi: 10.1029/2009JF001305

STUMP, E. & FITZGERALD, P. G. 1992. Episodic uplift of the Transantarctic Mountains. *Geology*, **20**, 161–164.

STUMP, E., GOOTEE, B. F. & TALARICO, F. 2005. Tectonic model for the Byrd glacier discontinuity and surrounding regions of the Transantarctic Mountains during the Neoproterozoic-early Paleozoic. *In*: FUTTERER, D. K., DAMASKE, D., KLEINSCHMIDT, G., MILLER, H. & TESSENSOHN, F. (eds) *Antarctica: Contributions to Global Earth Sciences*. Springer, Berlin, 179–188.

VAN SOEST, M. C., HODGES, K. V. *ET AL.* 2011. (U–Th)/He dating of terrestrial impact structures: the Manicouagan example. *Geochemistry, Geophysics, Geosystems*, **12**, Q0AA16, doi: 10.1029/2010GC003465.

YORK, D. 1969. Least-squares fitting of a straight line. *Canadian Journal of Physics*, **44**, 1079–1086.

ZEITLER, P. K., HERCZIG, A. L., MCDOUGALL, I. & HONDA, M. 1987. U–Th–He dating of apatite: a potential thermochronometer. *Geochimica et Cosmochimica Acta*, **51**, 2865–2868.